European Journal of Medicinal Chemistry 136 (2017) 348–359

Contents lists available at ScienceDirect

European Journal of Medicinal Chemistry

journal homepage: http://www.elsevier.com/locate/ejmech

Research paper

Design, synthesis and biological evaluation of uncharged catechol derivatives as selective inhibitors of PTP1B

Xiang-Qian Li [a, b, 1], Qi Xu [a, b, c, 1], Jiao Luo [a, b, c], Li-Jun Wang [a, b], Bo Jiang [a, b], Ren-Shuai Zhang [a, b], Da-Yong Shi [a, b, c, *]

[a] Key Laboratory of Experimental Marine Biology, Institute of Oceanology, Chinese Academy of Sciences, Qingdao, China
[b] Laboratory for Marine Drugs and Bioproducts, Qingdao National Laboratory for Marine Science and Technology, Qingdao, China
[c] University of Chinese Academy of Sciences, Beijing, China

ARTICLE INFO

Article history:
Received 19 January 2017
Received in revised form
27 April 2017
Accepted 2 May 2017
Available online 3 May 2017

Keywords:
Type 2 diabetes
PTP1B inhibition
Selectivity
Competitive
Cellular activity

ABSTRACT

Protein tyrosine phosphatases 1B (PTP1B) is a promising and validated therapeutic target to effectively treat T2DM and obesity. However, the development of charged PTP1B inhibitors was restricted due to their low cell permeability and poor bioavailability. Based on active natural products, two series of uncharged catechol derivatives were identified as PTP1B inhibitors by targeting a secondary aryl phosphate-binding site as well as the catalytic site. The most potent inhibitor **22** showed an IC_{50} of 0.487 μM against PTP1B and strong selectivity (27-fold) over TCPTP. Kinetic studies were also performed that **22** act as a competitive PTP1B inhibitor. The treatment of C2C12 myotubes with **22** markedly increased the phosphorylation levels of IRβ, Akt and IRS1 phosphorylation. The similarity of its action profiling with that produced by insulin suggested its potential as a new non-insulin-dependent drug candidate.

1. Introduction

Protein tyrosine phosphatases 1B (PTP1B), a member of PTPs family, is a key negative regulator in both insulin and leptin signaling pathways [1,2]. It can down regulate insulin signaling by dephosphorylating the insulin receptor and several of its downstream signaling proteins [3,4], thereby modulates both glucose and lipid metabolism. PTP1B knockout mice displayed enhanced insulin sensitivity, lower plasma glucose and insulin levels, without causing abnormalities in growth or other vital functions [5,6]. Hence, PTP1B is considered as a promising drug target for the treatment of type 2 diabetes and obesity.

Accordingly, various PTP1B inhibitors, difluoromethylene phosphonate [7,8] and carboxylic acid pTyr mimetic [9,10], have been developed extensively over the past decade. However, the limited cell membrane permeability failed to support them to progress beyond pre-clinical stage [11–13], owing to the highly charged pharmacophore that were incorporated to achieve an adequate binding affinity. Non-acid-containing ligands targeting site B are highly desirable for improving the overall druglike properties.

To increase selectivity versus highly homologous T-cell PTP (TCPTP) is another great challenge for the design of PTP1B inhibitors. T-Cell PTP (TCPTP) is highly homologous to PTP1B, with 74% sequence identity in the catalytic region [14,15]. Unlike the PTP1B knockout mice that develop normally, the TCPTP knockout died within 3–5 weeks after birth, because of the defects in hematopoiesis and immune function caused by abnormalities in B- and T-cells [15]. Simultaneous inhibition of PTP1B and TCPTP is considered unsuitable.

Some PTP1B inhibitors with good selectivity over TCPTP (20-fold) had been reported successively in the last decade [14,16–18]. However, most of them were acid-containing compounds without cell activity studies and following reports. Non-acid-containing inhibitors, such as (S)-isothiazolidinone derivatives, showed high affinity for PTP1B ($IC_{50} = 0.055$ μM) and low cellular activity, but exhibited no selectivity over TCPTP [19,20]. Hence, there is an urgent need to develop small molecule PTP1B inhibitors devoid of any charged moieties and with good selectivity.

In the last few years, we have identified a series of bromophenol PTP1B inhibitors from the ethanolic extract of the red alga

* Corresponding author. Key Laboratory of Experimental Marine Biology, Institute of Oceanology, Chinese Academy of Sciences, Qingdao, China.
E-mail address: shidayong@qdio.ac.cn (D.-Y. Shi).
[1] These authors contributed equally to this work.

http://dx.doi.org/10.1016/j.ejmech.2017.05.007
0223-5234/

rhodomela confervoides (Fig. 1) [21,22]. These natural products with an uncharged catechol have shown hypoglycemic effect mediated by PTP1B inhibition over few in vitro and in vivo diabetic and obese models. Furthermore, some other groups reported that many natural PTP1B inhibitors with the catechol pharmacophore from *Broussonetia papyrifera* [23], *Licorice* [24], *Tradescantia spathacea Sw.* [25], *Phellinus igniarius* [26], also showed moderate inhibitory activities against PTP1B (Fig. 1).

In this context, the catechol that these active natural products have in common was proposed as a lead to guide molecular design of novel PTP1B inhibitors. Prompted by these findings, two series of catechol derivatives were prepared and their inhibitory activity against the PTP1B enzyme was assessed. The results from the binding assays were also used to re-evaluate the docking results in order to gain insight into their possible binding modes, allowing the development of more active compounds in the future.

2. Results and discussion

2.1. Chemistry

The designed compounds were synthesized according to the general method depicted in Scheme 1. The synthesis began with 3,4-dihydroxybenzoic acid to afford the requisite intermediate 4-(5-mercapto-1,3,4-oxadiazol-2-yl)benzene-1,2-diol through a long synthetic sequence included esterification, hydrazinolysis and cyclization reactions [27]. After alkylation with chloracetates or α-bromoacetophenones, intermediate 4-(5-mercapto-1,3,4-oxadiazol-2-yl)benzene-1,2-diol were converted to target compounds **2**–**18**.

The preparation of 2,5-disubstituted oxazole derivatives (**19**–**27**) also required a long synthetic sequence included bromination, amination and cyclization reactions (Scheme 2). Initially, variously substituted acetophenones have been synthesized by copper-catalyzed Ullmann diaryl ether synthesis [28] and were bromination by copper(II) bromide in refluxing chloroform-ethyl acetate [29]. Intermediate α-bromoacetophenone were reacted with hexamethylenetetramine, and then hydrolyzed by 4 M HCl/EtOH to afford α-aminoacetophenone [30]. The synthesis of target 2,5-disubstituted was achieved in the presence of iodine and TBHP from α-aminoketone and aromatic aldehydes [31].

2.2. Structure-based design of PTP1B inhibitors

PTP1B enzyme contains two aryl phosphate-binding sites: a high affinity catalytic site (site A) and the second phosphotyrosine binding site (site B). The collective interactions with both sites are proposed to increase the inhibitory activity for PTP1B and enhance the selectivity over TCPTP [32,33]. Previous research suggested that a such inhibitor of PTP1B may require a combination of four moieties: a hydrophilic head, an aromatic center, a linker and a hydrophobic tail (Fig. 2) [32]. A hydrophilic head was proposed to occupy the catalytic site of PTP1B enzyme through hydrogen bonds with the residues Ser216, Ile219, Gly220 and Arg221, which embrace the catalytic residue Cys215. The aromatic center was designed to participate in extensive van der Waals interactions with Tyr46, Val49, Ile219, and F182 of the flap [19,34,35]. An appropriate linker could pass through the "gateway" region to access the site B from the site A [36]. Hydrophobic substituents of different sizes were employed to occupy site B, especially the residue Ala27 that is related to selectivity.

3,4-dihydroxybenzaldehyde (**1**) with a catechol core was selected as the hydrophilic head to occupy site A. PTP1B inhibitory assay of our own laboratory identified that compound **1** exhibited weak inhibitory activity (29% inhibition at 1 mM, not shown). As shown in Fig. 3a, the catechol core is accommodated in the catalytic site of PTP1B enzyme through a network of hydrogen bonds with the residues Ser216, Ile219, Gly220 and Arg221. Such interactions do have great influence on the catalytic function of PTP1B, but inhibitory activity still need to be improved by adding pharmacophore to occupy other binding site. Therefore, the second phosphotyrosine binding site (site B) was selected to offer opportunities for both potency and selectivity improvement.

Subsequently, an oxadiazole ring was introduced as an aromatic center and a corner structure, which could pass through the "gateway" between site A and site B. Compounds **2**–**5** were obtained by introducing hydrophobic substitution groups into the terminal and determined to inhibit PTP1B with IC_{50} values of 8.09–35.58 μM respectively (Table 1). As expected, these compounds maintain the binding mode of **1**, the additional groups lie along the tunnel wall and offer a favorable trajectory toward the B site, as shown in Fig. 3b and c, respectively.

With a purpose to improve the potency of **4** and **5**, further optimization was attempted by introducing different hydrophobic substituents into their para-position of the terminal phenyl ring.

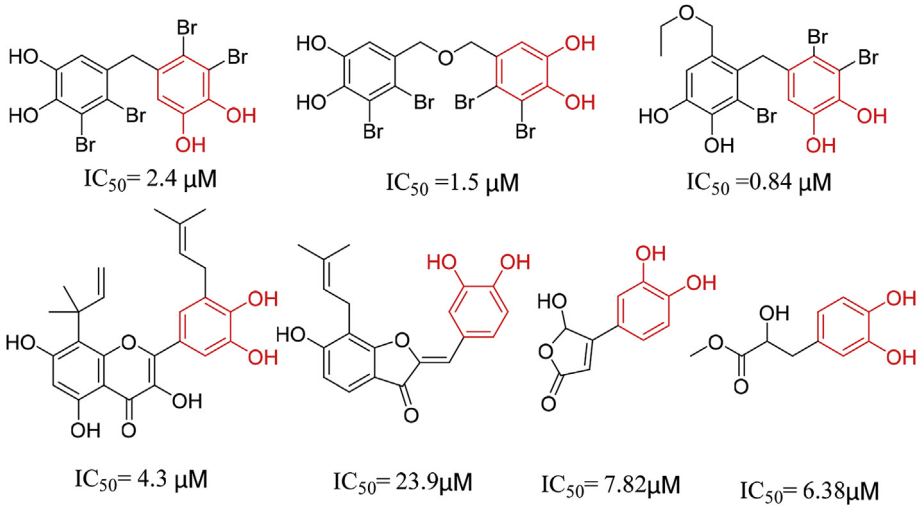

Fig. 1. Representative natural PTP1B Inhibitors with the catechol pharmacophore.

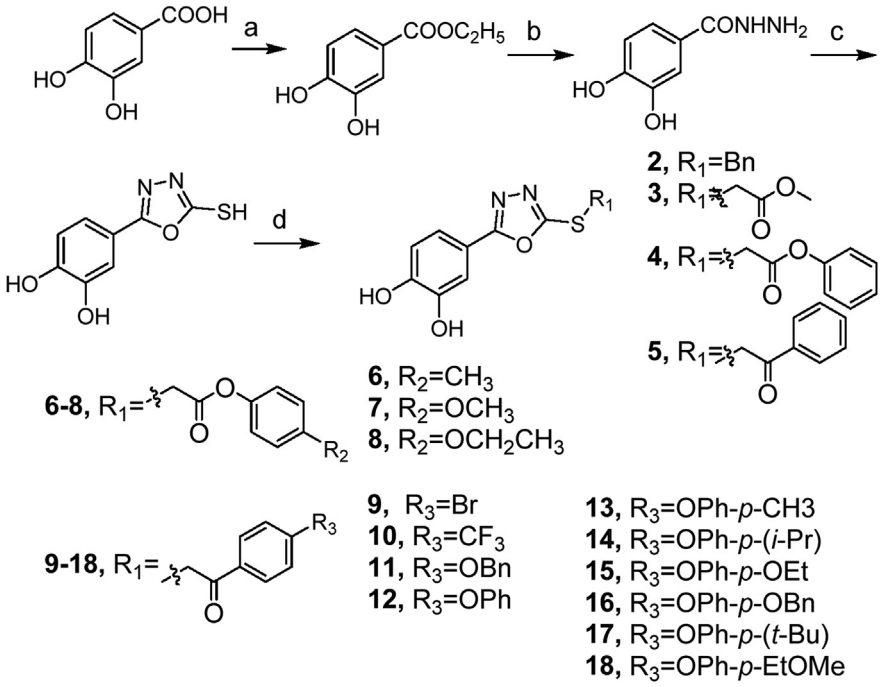

Scheme 1. Synthesis of designed compounds. Reagents and conditions: (a) H_2SO_4, EtOH, reflux, 4 h; (b) $N_2H_4 \cdot H_2O$ (85%, 6.0 equiv), EtOH, reflux, 6 h; (c) CS_2 (2.3 equiv), KOH (1.0 equiv), EtOH, reflux, 4 h; (d) KOH (1.0 equiv), Cl-R_1 or Br-R_1 (1.0 equiv), EtOH, H_2O, rt, 1 h.

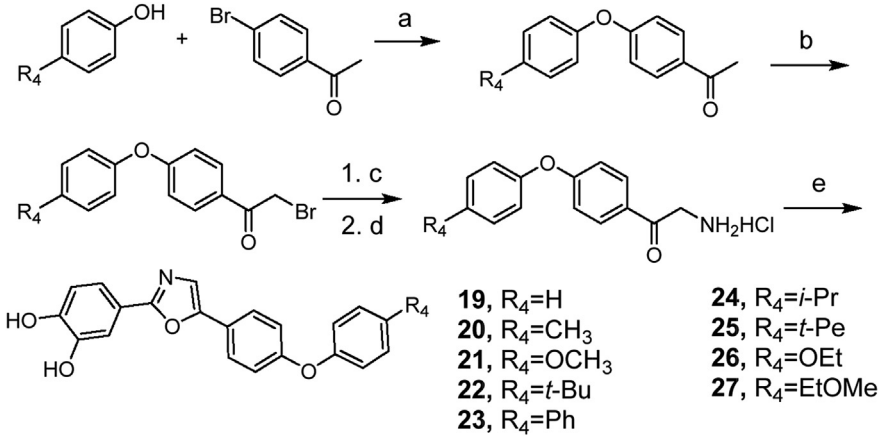

Scheme 2. Synthesis of designed compounds. Reagents and conditions: (a) CuI (0.1 equiv), K_2CO_3 (1.2 equiv), DMF, 140 °C, 14 h; (b) $CuBr_2$ (2.0 equiv), $CHCl_3$, EtOAc, reflux, 2 h; (c) $(CH_2)_6N_4$ (1.0 equiv), $CHCl_3$, 2 h; (d) HCl (35%, 5.0 equiv), EtOH, rt, 48 h; (e) 3,4-dihydroxybenzaldehyde (1.0 equiv), I_2 (0.15 equiv), TBHP (1.0 equiv), DMF, $NaHCO_3$ (1.0 equiv), 70 °C, 10 h.

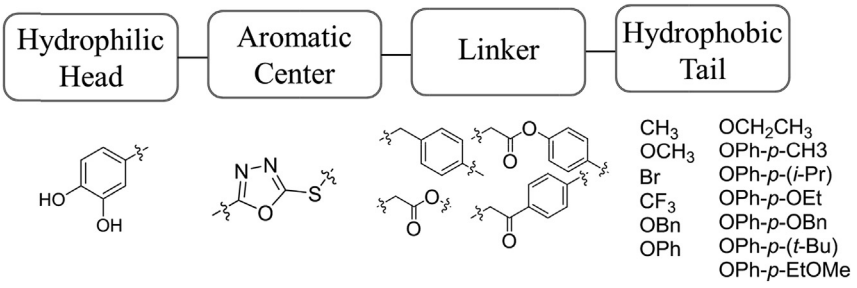

Fig. 2. Design of catechol derivatives as novel PTP1B inhibitors.

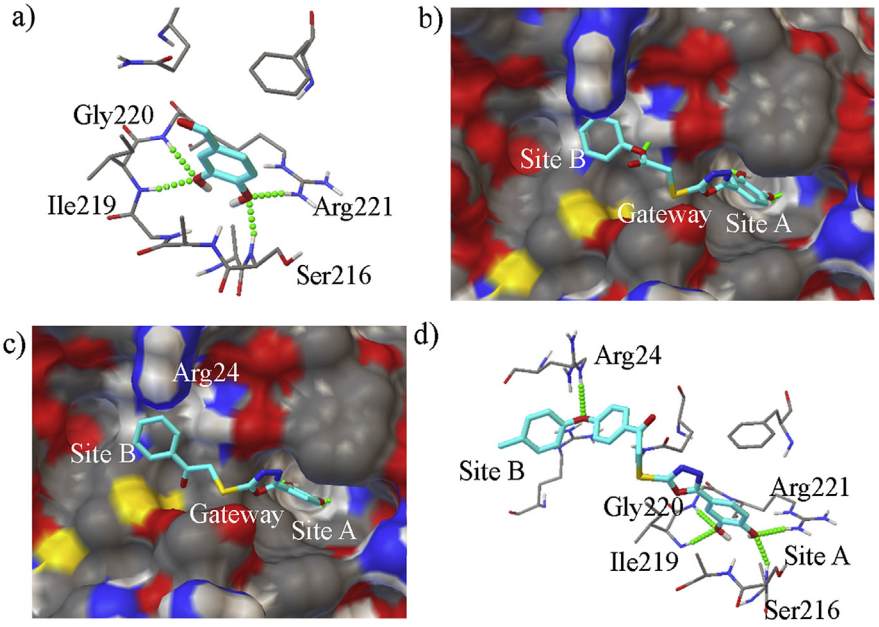

Fig. 3. Predicted binding models of PTP1B (1G1H) with (a) compound **1**; (b) compound **4**; (c) compound **5** (d) compound **13**. Carbon, oxygen, nitrogen, bromine, and sulfur atoms are colored gray 9(light blue), red, blue, green, and yellow, respectively. Hydrogen bonds are depicted as green lines. (For interpretation of the references to colour in this figure legend, the reader is referred to the web version of this article.)

Table 1
In vitro inhibitory activity of designed compounds **2**–**5** to PTP1B.

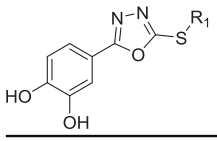

Compd	R_1	PTP1B IC_{50}±SD (μM)
2		31.63 ± 2.6
3		35.58 ± 4.8
4	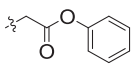	8.09 ± 2.1
5	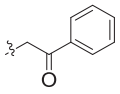	15.49 ± 4.3
Sodium vanadate		3.09 ± 0.13

Two series of compounds, **6**–**8** and **9**–**18**, were synthesized and showed improved PTP1B inhibitory activity (Table 2). Interestingly, when introducing methyl group on para-position of phenyl group (**6** and **13**) inhibited PTP1B with similar IC_{50} values, 4.74 μM and 3.89 μM, respectively.

Docking studies showed that compound **13** do not only form a network of H-bonds with Ser216, Ile219, Gly220 and Arg221, but also form an O•••H-N hydrogen bond with the positive charged side chain of Arg24 (2.052 Å, Fig. 3d). The terminal *p*-methyl lies on a small hydrophobic pocket formed by the main- and side-chain atoms of Met258, Gly259 and Ala27, which cannot accommodate a larger group.

2.3. Entropy-driven optimization of PTP1B inhibitors

Ligand binding is a multistep process that involves the desolvation and conformational rearrangement of both the ligand and the binding site [37]. Correspondingly, entropy-driven optimization by adding lipophilic moieties and applying chain-ring strategies are successful tools routinely used in medicinal chemistry programs [37–39]. More lipophilic compounds desolvate more easily, resulting in a significant reward in desolvation entropy [40]. However, repeated attempts to increase hydrophobic on para-position of terminal phenyl group (compound **6**–**18**) did not translate into expected inhibitory activity improvement in our study. Therefore, entropy-driven optimization by applying chain-ring became the strategy of further study (compound **19**–**27**, Fig. 4). Reducing ligand flexibility by limiting its rotational freedom could decrease the penalty arising from conformational entropy changes.

Encouraged by the above findings, a series of oxazole compounds (**19**–**27**), with rigid structure and lipophilic groups, were designed and synthesized. The results (shown in Table 3) indicated that all of these compounds showed potential inhibitory activity toward PTP1B. The presence of the methyl group give compound **20** improved inhibitory activity against PTP1B (IC_{50} = 0.809 μM). Amazingly, when *t*-butyl was incorporated to para-position, inhibitory activity had obvious improvement (**22**, IC_{50} = 0.487 μM). The molecular modeling (Fig. 5) predicted that compound **20** and **22** maintain the similar binding modes, occupying both site A and site B simultaneously. The additional lipophilic groups fill a hydrophobic cavity, which is formed by the main- and side-chain atoms of Met258, Gly259, Arg254 and Ala27.

2.4. Selectivity over TCPTP

Since Ala27 is not conserved between PTP1B and TCPTP, interaction with Ala27 had the potential to impart selectivity to PTP1B inhibitors [33]. Our molecular modeling predicted that several potent compounds **7**, **13**, **22** and **23** interact with Ala27 in an edge-

Table 2
In vitro inhibitory activity of designed compounds **6**–**18** to PTP1B.

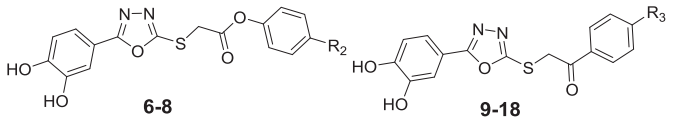

Compd	Group R_2 or R_3	PTP1B IC_{50}±SD (μM)	Compd	Group R_2 or R_3	PTP1B IC_{50}±SD (μM)
6	R_2 = CH3	4.74 ± 0.9	**13**	R_3 = OPh-*p*-CH_3	3.89 ± 0.8
7	R_2 = OCH3	6.02 ± 1.5	**14**	R_3 = OPh-*p*-(*i*-Pr)	10.96 ± 3.1
8	R_2 = OCH_2CH_3	7.94 ± 1.1	**15**	R_3 = OPh-*p*-OEt	16.98 ± 2.3
9	R_3 = Br	115.34 ± 8.6	**16**	R_3 = OPh-*p*-OBn	21.37 ± 3.7
10	R_3 = CF_3	21.38 ± 3.2	**17**	R_3 = OPh-*p*-(t-Bu)	10.47 ± 1.9
11	R_3 = OBn	7.79 ± 1.8	**18**	R_3 = OPh-*p*-EtOMe	22.75 ± 3.4
12	R_3 = OPh	9.33 ± 2.2	Sodium vanadate		3.09 ± 0.13

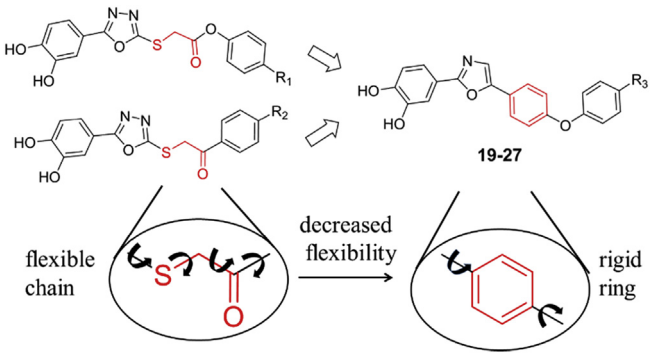

Fig. 4. Entropy-driven optimization by applying chain-ring strategy.

Table 3
In vitro inhibitory activity of designed compounds **19**–**27** to PTP1B.

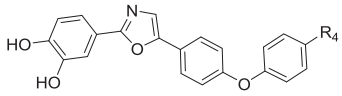

Compd	Group R_4	PTP1B IC_{50}±SD (μM)
19	H	2.63 ± 0.7
20	CH_3	0.807 ± 0.21
21	OCH_3	6.92 ± 1.3
22	*t*-Bu	0.487 ± 1.3
23	Ph	6.25 ± 1.7
24	*i*-Pr	7.44 ± 3.9
25	*t*-Pe	3.60 ± 1.3
26	OEt	20.82 ± 3.6
27	EtOMe	19.14 ± 6.7
Sodium vanadate		3.09 ± 0.13

to-edge fashion. The in vitro selectivity over TCPTP was evaluated for these four compounds, using pNPP assay and IC_{50} values in Table 4. Compounds **7** and **22** showed 16–27-fold selectivity, **13** showed about 2-fold selectivity, while **23** showed no selectivity over TCPTP enzyme. The introduction of the methoxyl and *t*-butyl substituents might force an interaction with Ala27 in PTP1B, which are less tolerated by the larger replacement (Ser29) at this position in TCPTP. Ser29 might push the methoxyl and *t*-butyl substituents to a different and presumably less favorable conformation.

2.5. Kinetic studies

To elucidate the inhibition modes of compounds **20** and **22** with strong inhibitory activity against PTP1B, kinetic analyses were performed (Fig. 6). Various concentrations of pNPP (0.5, 1.0, 2.0, 4.0, and 8.0 mM) were used as a PTP1B substrate in the absence or presence of compounds. The effects of compounds **12** and **22** on the kinetic profile of PTP1B-catalyzed pNPP hydrolysis were investigated as described in methods. As the graph showed straight lines intersected each other on the 1/v axis, compounds **12** and **22** behaved as competitive inhibitors, indicating that they may bind at the active site of the PTP1B enzyme.

2.6. Cellular activity

Insulin signal transduction initiates when the insulin binds to the insulin receptor (IR), which stimulates IR intrinsic kinase activity and activates a number of downstream molecules including insulin receptor substrate 1 (IRS1) and Akt by phosphorylation, in turn, lead to increased influx of glucose into the skeletal muscle cells [41–43]. Hence, phosphorylation of the signaling molecules plays a vital role in the activation of insulin signaling pathway. PTP1B serves as a negative regulator of the insulin activated signaling pathways, inhibition of which could up-regulate phosphorylation levels of insulin receptor β (IRβ), insulin receptor substrate 1 (IRS-1) and protein kinase B (Akt).

Given the observed potency of **22** for PTP1B, we next explored its possible regulatory role in IRβ, IRS-1 and AKT activation. As shown in Fig. 7, incubation of C2C12 cells with **22** in 0.5, 1, 2, 4 μM concentration range increased insulin-mediated IRβ, IRS-1 and AKT phosphorylation levels compared to controls. The uptake levels determined at 2 μM concentration were comparable to that produced by insulin (100 nM). These results suggest that **22** possesses good membrane permeability, and could possibly induce insulin signaling at the cellular level.

3. Conclusion

Two series of uncharged catechol derivatives were synthesized and identified as competitive PTP1B inhibitors. Among them, the representative compound **22** had strong inhibitory activity to PTP1B (IC_{50} = 0.487 μM) and exhibited good specificity for PTP1B over TCPTP (27-fold). Further studies on cellular activities revealed that **22** was membrane-permeable and exerted non-insulin-dependent cellular effects on the activation of IRβ, IRS-1 and Akt pathway in C2C12 myotubes at a concentration of 2.0 μM.

These results provide further evidence that non-acid-containing catechol derivatives can be potent inhibitor of PTP1B with high selectivity over TCPTP and non-insulin-dependent cellular activity. A hydrophilic head incorporating a hydrophobic tail provide new opportunity to overcome two challenges for the design of PTP1B

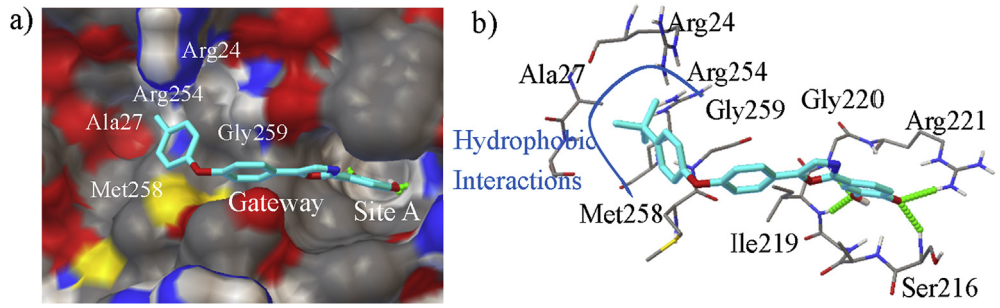

Fig. 5. Predicted binding models of PTP1B (1G1H) with (a) compound **20** and (b) compound **22**. Carbon, oxygen, nitrogen, bromine, and sulfur atoms are colored gray (light blue), red, blue, green, and yellow, respectively. Hydrogen bonds are depicted as green lines. Hydrophobic interaction is labeled by blue line. (For interpretation of the references to colour in this figure legend, the reader is referred to the web version of this article.)

Table 4
Selectivity ratios for the compounds designed to interact with Ala27.

Compounds	7	13	22	23
Terminal groups	OMe	Me	*t*-Bu	Ph
PTP1B (IC_{50}, μM)	6.02 ± 1.3	3.89 ± 0.67	0.487 ± 0.38	6.25 ± 1.36
TCPTP (IC_{50}, μM)	>100	8.73 ± 2.14	13.31 ± 2.55	5.01 ± 1.34
Selectivity[a]	16.6	2.24	27.34	0.80

[a] TCPTP IC_{50}/PTP1B IC_{50}.

inhibitors, selectivity and membrane-permeable. These compounds will provide new insights into the design and development of non-insulin-dependent agents to treat type 2 diabetes.

4. Experimental section

4.1. Chemistry

All commercial reagents were purchased and used without further purification or distillation unless otherwise stated. Melting points were measured on a Griffin apparatus and are uncorrected. NMR (^1H, ^{13}C) was obtained with Bruker AV-500 spectrometer with chemical shifts reported as parts per million (TMS as internal standard). The following abbreviations are used for multiplicity of NMR signals: s = singlet, d = doublet, t = triplet, q = quartet, m = multiplet. Column chromatography was performed on silica gel 200–300 mesh. Purity of all final products was determined by analytical HPLC to be >95%. HPLC purity of compounds was measured with a normal phase HPLC (XBridge C18, 4.6 × 150 mm, 5 μm) with two diverse wavelength detection systems. Compounds were eluted using a gradient elution of 40/60 to 0/100H_2O/CH_3OH over 30 min at a flow rate of 1.0 mL/min.

4.2. General procedure for the preparation of 4-(5-mercapto-1,3,4-oxadiazol-2-yl)benzene-1,2-diol

To a solution of 3,4-dihydroxybenzoic acid (15.4 g, 0.1 mol) in absolute ethanol (200 mL) was added 5 mL concentrated sulfuric acid. This mixture was heated at reflux for 4 h. After cooling to ambient temperature, water (100 mL) was slowly introduced over a period of 10 min. The mixture was extracted with EtOAc, washed with diluted HCl followed by water, dried with Na_2SO_4. Then solvent was removed under reduced pressure, the yellow powder as ethyl 3,4-dihydroxybenzoate was used without further disposal. Yield 15.8 g, 86.8%.

The crude product (15.8 g, 0.087 mol) were dissolved in ethanol (100 mL) and 37.5 g $N_2H_4.H_2O$ were dropwise added. The mixture was refluxed for 6 h. After cooling to room temperature, the

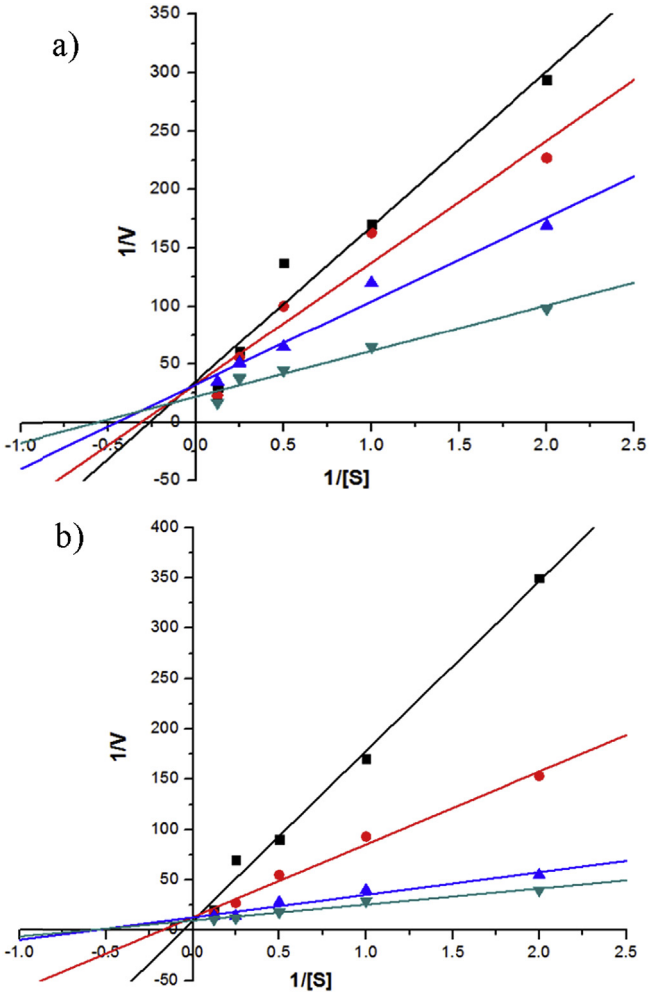

Fig. 6. The effect of **20** and **22** on PTP1B-catalyzed pNPP hydrolysis. (a) **20** concentrations were 1, 2, 4, and 8 μM, respectively. (b) **22** concentrations were 0, 1, 2, and 4 μM, respectively. The experiment was performed at 37 °C and pH 7.0.

reaction mixture was diluted with cold water and acidified with 1 M HCl. The precipitated solid was filtered and washed with water to obtain 3,4-dihydroxybenzohydrazide hydrochloride (12.0 g, 88.9%), which was used in the next step without further purification.

A solution of 12.0 g (0.071 mol) of the 3,4-dihydroxybenzohydrazide and 4.0 g (0.072 mol) KOH in absolute ethanol (200 mL) was treated to the addition of carbon disulfide

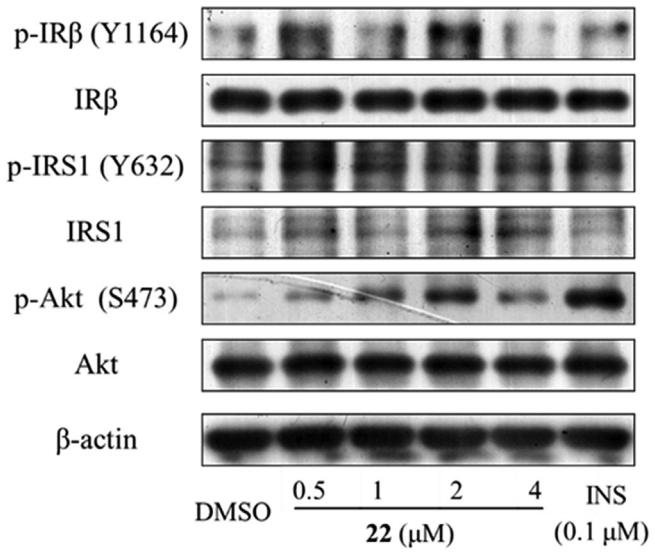

Fig. 7. Activation of insulin signaling during exposure of C2C12 myotubes to **22**. C2C12 myotubes were treated with **22** in 0.5, 1, 2, 4 μM concentration range or 100 nM insulin for 30 min in serum-free DMEM. Then, phosphorylation levels of IRβ, IRS-1 and Akt were determined by immunoblotting.

(12 g, 0.162 mol). This mixture was heated at reflux for 4 h. After cooling to ambient temperature, concentrated hydrochloric acid (20 mL) was slowly introduced causing the precipitation of a light yellow solid, 4-(5-mercapto-1,3,4-oxadiazol-2-yl)benzene-1,2-diol (10.3 g, 69.1%).

4.3. General procedure for the preparation of **2**–**18**

A mixture of 4-(5-mercapto-1,3,4-oxadiazol-2-yl)benzene-1,2-diol (105 mg, 0.5 mmol), KOH (20 mg, 0.5 mmol) in 10 mL H_2O was stirred vigorously under nitrogen for 1 h at room temperature. Under vigorous stirring, chloroacetate or bromoacetophenone (0.5 mmol) in 20 mL ethanol was slowly added to the mixture. After 1 h, water was slowly added with rapid stirring under ice-water bath. Crystals were obtained after filtration and purified by silica gel flash column chromatography (CH_2Cl_2/acetone = 35:1).

4.3.1. 4-(5-(Benzylthio)-1,3,4-oxadiazol-2-yl)benzene-1,2-diol (**2**)

M.p. 178.8–179.2 °C. ^{1}H NMR (500 MHz, DMSO-d_6) δ 9.79 (s, 1H), 9.52 (s, 1H), 7.43 (d, J = 7.4 Hz, 2H), 7.36–7.29 (m, 3H), 7.26 (d, J = 7.4 Hz, 1H), 7.23 (d, J = 8.2 Hz, 1H), 6.86 (d, J = 8.2 Hz, 1H), 4.51 (s, 2H). ^{13}C NMR (126 MHz, DMSO-d_6) δ 165.95 (s), 162.36 (s), 149.79 (s), 146.30 (s), 137.08 (s), 129.43 (s), 129.01 (s), 128.17 (s), 119.09 (s), 116.63 (s), 114.30 (s), 113.71 (s), 36.39 (s). DEPT (135°) δ 129.43 (CH), 129.01 (CH), 128.17 (CH), 119.09 (CH), 116.63 (CH), 113.70 (CH), 36.38 (negative peak, CH_2). DEPT (90°) δ 129.43 (CH), 129.01 (CH), 128.17 (CH), 119.09 (CH), 116.63 (CH), 113.70 (CH). HRMS (ESI+) m/z: 323.0461 (M + Na). HPLC purity = 99.019%, t_R = 4.725 min.

4.3.2. Methyl 2-((5-(3,4-dihydroxyphenyl)-1,3,4-oxadiazol-2-yl) thio)acetate (**3**)

M.p. 158.2–160.9 °C. ^{1}H NMR (500 MHz, DMSO-d_6) δ 9.78 (s, 1H), 9.57 (s, 1H), 7.30 (s, 1H), 7.23 (d, J = 8.2 Hz, 1H), 6.87 (d, J = 8.2 Hz, 1H), 4.23 (s, 2H), 3.67 (s, 3H). ^{13}C NMR (126 MHz, DMSO-d_6) δ 168.76 (s), 165.98 (s), 162.02 (s), 149.84 (s), 146.31 (s), 119.10 (s), 116.65 (s), 114.20 (s), 113.70 (s), 53.17 (s), 34.10 (s). DEPT (135°) δ 119.09 (CH), 116.65 (CH), 113.69 (CH), 53.16 (CH_3), 34.09 (negative peak, CH_2). DEPT (90°) δ 119.10 (CH), 116.65 (CH), 113.70 (CH). HRMS (ESI+) m/z: 305.0207 (M + Na). HPLC purity = 99.255%, t_R = 4.024 min.

4.3.3. Phenyl 2-((5-(3,4-dihydroxyphenyl)-1,3,4-oxadiazol-2-yl) thio)acetate (**4**)

M.p. 119.2–120.6 °C. ^{1}H NMR (500 MHz, DMSO-d_6) δ 9.82 (s, 1H), 9.54 (s, 1H), 7.41 (t, J = 7.7 Hz, 2H), 7.33 (s, 1H), 7.26 (overlap, 2H), 7.11 (d, J = 8.2 Hz, 2H), 6.87 (d, J = 8.2 Hz, 1H), 4.50 (s, 2H). ^{13}C NMR (126 MHz, DMSO-d_6) δ 167.39 (s), 166.15 (s), 161.95 (s), 150.80 (s), 149.89 (s), 146.34 (s), 130.11 (s), 126.66 (s), 121.84 (s), 119.15 (s), 116.65 (s), 114.18 (s), 113.75 (s), 34.48 (s). DEPT (135°) δ 130.11 (CH), 126.66 (CH), 121.84 (CH), 119.15 (CH), 116.65 (CH), 113.75 (CH), 34.47 (negative peak, CH_2). DEPT (90°) δ 130.11 (CH), 126.66 (CH), 121.84 (CH), 119.15 (CH), 116.65 (CH), 113.75 (CH). HRMS (ESI+) m/z: 367.0372 (M + Na). HPLC purity = 99.883%, t_R = 4.25 min.

4.3.4. 2-((5-(3,4-Dihydroxyphenyl)-1,3,4-oxadiazol-2-yl)thio)-1-phenylethan-1-one (**5**)

M.p. 216.3–218.2 °C. ^{1}H NMR (500 MHz, DMSO-d_6) δ 9.78 (s, 1H), 9.52 (s, 1H), 8.04 (d, J = 7.5 Hz, 2H), 7.69 (t, J = 7.4 Hz, 1H), 7.56 (t, J = 7.7 Hz, 2H), 7.30 (s, 1H), 7.21 (d, J = 8.2, 1H), 6.85 (d, J = 8.2 Hz, 1H), 5.11 (s, 2H). ^{13}C NMR (126 MHz, DMSO-d_6) δ 193.17 (s), 165.85 (s), 162.39 (s), 149.78 (s), 146.30 (s), 135.48 (s), 134.42 (s), 129.34 (s), 128.91 (s), 119.08 (s), 116.61 (s), 114.28 (s), 113.70 (s), 40.89 (s). DEPT (135°) δ 134.42 (CH), 129.34 (CH), 128.91 (CH), 119.08 (CH), 116.61 (CH), 113.70 (CH), 40.88 (negative peak, CH_2). DEPT (90°) δ 134.41 (CH), 129.34 (CH), 128.90 (CH), 119.08 (CH), 116.60 (CH), 113.69 (CH). HRMS (ESI+) m/z: 351.0416 (M + Na). HPLC purity = 98.959%, t_R = 4.375 min.

4.3.5. p-Tolyl 2-((5-(3,4-dihydroxyphenyl)-1,3,4-oxadiazol-2-yl) thio)acetate (**6**)

M.p. 156.9–158.1 °C. ^{1}H NMR (500 MHz, DMSO-d_6) δ 9.87 (s, 1H), 9.59 (s, 1H), 7.32 (s, 1H), 7.25 (d, J = 8.2 Hz, 1H), 7.19 (d, J = 8.2 Hz, 2H), 6.97 (d, J = 8.2 Hz, 2H), 6.87 (d, J = 8.2 Hz, 1H), 4.46 (s, 2H), 2.26 (s, 3H). ^{13}C NMR (126 MHz, DMSO-d_6) δ 167.49 (s), 166.13 (s), 161.99 (s), 149.87 (s), 148.58 (s), 146.32 (s), 135.91 (s), 130.42 (s), 121.50 (s), 119.18 (s), 116.64 (s), 114.16 (s), 113.72 (s), 34.42 (s), 20.80 (s). DEPT (135°) δ 130.41 (CH), 121.50 (CH), 119.18 (CH), 116.63 (CH), 113.72 (CH), 34.42 (negative peak, CH_2), 20.80 (CH_3). DEPT (90°) δ 130.42 (CH), 121.50 (CH), 119.18 (CH), 116.64 (CH), 113.72 (CH). HRMS (ESI+) m/z: 381.0538 (M + Na). HPLC purity = 99.011%, t_R = 4.388 min.

4.3.6. 4-Methoxyphenyl 2-((5-(3,4-dihydroxyphenyl)-1,3,4-oxadiazol-2-yl)thio)acetate (**7**)

M.p. 183.3–183.9 °C. ^{1}H NMR (500 MHz, DMSO-d_6) δ 9.82 (s, 1H), 9.54 (s, 1H), 7.32 (s, 1H), 7.25 (d, J = 8.2 Hz, 1H), 7.02 (d, J = 8.9 Hz, 2H), 6.94 (d, J = 8.9 Hz, 2H), 6.87 (d, J = 8.2 Hz, 1H), 4.47 (s, 2H), 3.72 (s, 3H). ^{13}C NMR (126 MHz, DMSO-d_6) δ 167.65 (s), 166.12 (s), 161.96 (s), 157.52 (s), 149.88 (s), 146.33 (s), 144.18 (s), 122.65 (s), 119.15 (s), 116.65 (s), 115.00 (s), 114.18 (s), 113.74 (s), 55.87 (s), 34.43 (s). DEPT (135°) δ 122.65 (CH), 119.14 (CH), 116.64 (CH), 115.00 (CH), 113.74 (CH), 55.87 (CH_3), 34.42 (negative peak, CH_2). DEPT (90°) δ 122.65 (CH), 119.15 (CH), 116.64 (CH), 115.00 (CH), 113.74 (CH). HRMS (ESI+) m/z: 397.0493 (M + Na). HPLC purity = 95.141%, t_R = 5.251 min.

4.3.7. 4-Ethoxyphenyl 2-((5-(3,4-dihydroxyphenyl)-1,3,4-oxadiazol-2-yl)thio)acetate (**8**)

M.p. 151.2–152.4 °C. ^{1}H NMR (500 MHz, DMSO-d_6) δ 9.84 (s, 1H), 9.56 (s, 1H), 7.34 (s, 1H), 7.25 (d, J = 8.3 Hz, 1H), 7.00 (d, J = 8.9 Hz, 2H), 6.91 (d, J = 8.9 Hz, 2H), 6.88 (d, J = 8.3 Hz, 1H), 4.46 (s, 2H), 3.97 (q, J = 6.9 Hz, 2H), 1.28 (t, J = 6.9 Hz, 3H). ^{13}C NMR (126 MHz, DMSO-d_6) δ 167.65 (s), 166.13 (s), 161.97 (s), 156.79 (s), 149.89 (s), 146.34 (s), 144.06 (s), 122.63 (s), 119.15 (s), 116.66 (s), 115.44 (s), 114.18 (s),

113.76 (s), 63.83 (s), 34.42 (s), 15.03 (s). DEPT (135°) δ 122.63 (CH), 119.14 (CH), 116.66 (CH), 115.44 (CH), 113.76 (CH), 63.83 (negative peak, CH_2), 34.42 (negative peak, CH_2), 15.03 (CH_3). DEPT (90°) δ 122.63 (CH), 119.15 (CH), 116.66 (CH), 115.44 (CH), 113.76 (CH). HRMS (ESI+) *m/z*: 389.0828 (M + H). HPLC purity = 95.285%, t_R = 3.508 min.

*4.3.8. 1-(4-Bromophenyl)-2-((5-(3,4-dihydroxyphenyl)-1,3,4-oxadiazol-2-yl)thio)ethan-1-one (**9**)*

M.p. 236.6–237.6 °C. ^{1}H NMR (500 MHz, DMSO-d_6) δ 7.97 (d, *J* = 8.5 Hz, 2H), 7.78 (d, *J* = 8.5 Hz, 2H), 7.29 (s, 1H), 7.20 (d, *J* = 8.2 Hz, 1H), 6.85 (d, *J* = 8.2 Hz, 1H), 5.08 (s, 2H). ^{13}C NMR (126 MHz, DMSO-d_6) δ 192.56 (s), 165.90 (s), 162.26 (s), 149.83 (s), 146.32 (s), 134.51 (s), 132.42 (s), 130.90 (s), 128.59 (s), 119.08 (s), 116.60 (s), 114.23 (s), 113.69 (s), 40.74 (s). DEPT (135°) δ 132.41 (CH), 130.90 (CH), 119.08 (CH), 116.60 (CH), 113.69 (CH), 40.74 (negative peak, CH_2). DEPT (90°) δ 132.42 (CH), 130.90 (CH), 119.08 (CH), 116.60 (CH), 113.69 (CH). HRMS (ESI+) *m/z*: 328.9518 (M + Na). HPLC purity = 97.588%, t_R = 3.610 min.

*4.3.9. 2-((5-(3,4-Dihydroxyphenyl)-1,3,4-oxadiazol-2-yl)thio)-1-(4-(trifluoromethyl)phenyl)ethan-1-one (**10**)*

M.p. 237.4–238.3 °C. ^{1}H NMR (500 MHz, DMSO-d_6) δ 9.91 (s, 1H), 9.63 (s, 1H), 8.20 (d, *J* = 8.1 Hz, 2H), 7.91 (d, *J* = 8.1 Hz, 2H), 7.27 (s, 1H), 7.19 (d, *J* = 8.2 Hz, 1H), 6.84 (d, *J* = 8.2 Hz, 1H), 5.09 (s, 2H). ^{13}C NMR (126 MHz, DMSO-d_6) δ 192.83 (s), 165.94 (s), 162.28 (s), 149.78 (s), 146.24 (s), 138.62 (s), 133.45 (s), 129.71 (s), 126.32 (s), 126.29 (s), 119.16 (s), 116.58 (s), 114.18 (s), 113.66 (s), 40.72 (s). DEPT (135°) δ 129.71 (CH), 126.32 (CH), 126.29 (CH), 119.16 (CH), 116.58 (CH), 113.65 (CH), 109.99 (CH), 40.71 (negative peak, CH_2). DEPT (90°) δ 129.71 (s), 126.32 (CH), 126.29 (CH), 119.16 (s), 116.58 (s), 113.65 (s), 109.99 (CH). HRMS (ESI+) *m/z*: 419.0285 (M + Na). HPLC purity = 97.648%, t_R = 4.525 min.

*4.3.10. 1-(4-(Benzyloxy)phenyl)-2-((5-(3,4-dihydroxyphenyl)-1,3,4-oxadiazol-2-yl)thio)ethan-1-one (**11**)*

M.p. 218.7–220.8 °C. ^{1}H NMR (500 MHz, DMSO-d_6) δ 9.88 (s, 1H), 9.67 (s, 1H), 7.98 (d, *J* = 8.6 Hz, 2H), 7.42 (d, *J* = 7.2 Hz, 2H), 7.36 (t, *J* = 7.2 Hz, 2H), 7.31 (t, *J* = 7.1 Hz, 1H), 7.28 (s, 1H), 7.19 (d, *J* = 8.2 Hz, 1H), 7.12 (d, *J* = 8.6 Hz, 2H), 6.85 (d, *J* = 8.2 Hz, 1H), 5.17 (s, 2H), 4.98 (s, 2H). ^{13}C NMR (126 MHz, DMSO-d_6) δ 191.45 (s), 165.83 (s), 163.22 (s), 162.58 (s), 149.75 (s), 146.24 (s), 136.68 (s), 131.34 (s), 128.97 (s), 128.52 (s), 128.38 (s), 128.21 (s), 119.15 (s), 116.59 (s), 115.36 (s), 114.24 (s), 113.66 (s), 70.02 (s), 40.44 (s). DEPT (135°) δ 131.34 (CH), 128.96 (CH), 128.52 (CH), 128.21 (CH), 119.15 (CH), 116.59 (CH), 115.36 (CH), 113.66 (CH), 70.02 (negative peak, CH_2), 40.44 (negative peak, CH_2). HRMS (ESI+) *m/z*: 457.0834 (M + Na). HPLC purity = 96.448%, t_R = 3.840 min.

*4.3.11. 2-((5-(3,4-Dihydroxyphenyl)-1,3,4-oxadiazol-2-yl)thio)-1-(4-phenoxyphenyl)ethan-1-one (**12**)*

M.p. 189.6–191.2 °C. ^{1}H NMR (500 MHz, DMSO-d_6) δ 9.77 (s, 1H), 9.53 (s, 1H), 8.06 (d, *J* = 8.7 Hz, 2H), 7.45 (t, *J* = 7.8 Hz, 2H), 7.29 (s, 1H), 7.25 (t, *J* = 7.4 Hz, 1H), 7.20 (d, *J* = 8.2 Hz, 1H), 7.13 (d, *J* = 7.8 Hz, 2H), 7.06 (d, *J* = 8.7 Hz, 2H), 6.85 (d, *J* = 8.2 Hz, 1H), 5.05 (s, 2H). ^{13}C NMR (126 MHz, DMSO-d_6) δ 191.65 (s), 165.85 (s), 162.41 (s), 162.35 (s), 155.20 (s), 149.79 (s), 146.30 (s), 131.60 (s), 130.84 (s), 130.19 (s), 125.40 (s), 120.57 (s), 119.08 (s), 117.65 (s), 116.60 (s), 114.27 (s), 113.69 (s), 40.66 (s). DEPT (135°) δ 131.60 (CH), 130.84 (CH), 125.40 (CH), 120.57 (CH), 119.08 (CH), 117.65 (CH), 116.60 (CH), 113.69 (CH), 109.99 (CH), 40.66 (negative peak, CH_2). DEPT (90°) δ 131.60 (CH), 130.84 (CH), 125.40 (CH), 120.57 (CH), 119.08 (CH), 117.65 (CH), 116.59 (CH), 113.69 (CH), 109.99 (CH). HRMS (ESI+) *m/z*: 343.0683 (M + Na). HPLC purity = 95.787%, t_R = 3.302 min.

*4.3.12. 2-((5-(3,4-Dihydroxyphenyl)-1,3,4-oxadiazol-2-yl)thio)-1-(4-(p-tolyloxy)phenyl)ethan-1-one (**13**)*

M.p. 195.8–196.3 °C. ^{1}H NMR (500 MHz, DMSO-d_6) δ 8.04 (d, *J* = 8.2 Hz, 2H), 7.29 (s, 1H), 7.25 (d, *J* = 8.3 Hz, 2H), 7.20 (d, *J* = 8.2 Hz, 1H), 7.02 (overlap, 4H), 6.85 (d, *J* = 8.2 Hz, 1H), 5.04 (s, 2H), 2.30 (s, 3H). ^{13}C NMR (126 MHz, DMSO-d_6) δ 191.61 (s), 165.84 (s), 162.79 (s), 162.41 (s), 152.77 (s), 149.78 (s), 146.30 (s), 134.70 (s), 131.57 (s), 131.19 (s), 129.91 (s), 128.91 (s), 120.63 (s), 119.07 (s), 117.23 (s), 116.60 (s), 114.28 (s), 113.70 (s), 40.67 (s), 20.80 (s). DEPT (135°) δ 131.56 (CH), 131.19 (CH), 128.91 (CH), 120.63 (CH), 119.07 (CH), 117.22 (CH), 116.59 (CH), 113.69 (CH), 40.66 (negative peak, CH_2), 20.80 (CH_3). DEPT (90°) δ 131.57 (CH), 131.19 (CH), 129.34 (CH), 120.63 (CH), 119.07 (CH), 117.23 (CH), 116.60 (CH), 113.69 (CH). HRMS (ESI+) *m/z*: 457.0857 (M + Na). HPLC purity = 98.082%, t_R = 4.192 min.

*4.3.13. 2-((5-(3,4-Dihydroxyphenyl)-1,3,4-oxadiazol-2-yl)thio)-1-(4-(4-isopropylphenoxy)phenyl)ethan-1-one (**14**)*

M.p. 170.5–171.9 °C. ^{1}H NMR (500 MHz, DMSO-d_6) δ 8.05 (d, *J* = 8.6 Hz, 2H), 7.32 (s, 1H), 7.31–7.26 (m, 2H), 7.20 (d, *J* = 8.2, 1H), 7.04 (overlap, 4H), 6.85 (d, *J* = 8.2 Hz, 1H), 5.04 (s, 2H), 2.91 (m, 1H), 1.19 (d, *J* = 6.9 Hz, 6H). ^{13}C NMR (126 MHz, DMSO-d_6) δ 191.60 (s), 165.84 (s), 162.67 (s), 162.42 (s), 153.02 (s), 149.78 (s), 146.30 (s), 145.53 (s), 131.58 (s), 129.97 (s), 128.53 (s), 120.49 (s), 119.07 (s), 117.37 (s), 116.60 (s), 114.28 (s), 113.70 (s), 33.28 (s), 24.37 (s). DEPT (135°) δ 131.58 (CH), 128.53 (CH), 120.49 (CH), 119.07 (CH), 117.36 (CH), 116.59 (CH), 113.69 (CH), 40.66 (negative peak, CH_2), 33.28 (CH_3), 24.37 (CH_3). DEPT (90°) δ 131.58 (CH), 128.53 (CH), 120.49 (CH), 119.07 (CH), 117.36 (CH), 116.60 (CH), 113.69 (CH), 33.28 (CH). HRMS (ESI+) *m/z*: 485.1156 (M + Na). HPLC purity = 98.905%, t_R = 3.880 min.

*4.3.14. 2-((5-(3,4-Dihydroxyphenyl)-1,3,4-oxadiazol-2-yl)thio)-1-(4-(4-ethoxyphenoxy)phenyl)ethan-1-one (**15**)*

M.p. 217.3–218.1 °C.^{1}H NMR (500 MHz, DMSO-d_6) δ 9.79 (s, 1H), 9.51 (s, 1H), 8.03 (d, *J* = 8.6 Hz, 2H), 7.28 (s, 1H), 7.20 (d, *J* = 8.2 Hz, 1H), 7.06 (d, *J* = 8.6 Hz, 2H), 7.02–6.94 (m, 4H), 6.85 (d, *J* = 8.2 Hz, 1H), 5.03 (s, 2H), 4.01 (q, *J* = 6.9 Hz, 2H), 1.31 (t, *J* = 6.9 Hz, 3H). ^{13}C NMR (126 MHz, DMSO-d_6) δ 191.58 (s), 165.83 (s), 163.35 (s), 162.42 (s), 156.20 (s), 149.77 (s), 147.98 (s), 146.29 (s), 131.56 (s), 129.66 (s), 122.17 (s), 119.07 (s), 116.72 (s), 116.59 (s), 116.24 (s), 114.28 (s), 113.69 (s), 63.87 (s), 40.65 (s), 15.11 (s). DEPT (135°) δ 131.55 (CH), 122.17 (CH), 119.07 (CH), 116.72 (CH), 116.59 (CH), 116.24 (CH), 113.69 (CH), 109.99 (CH), 63.87 (negative peak, CH_2), 40.65 (negative peak, CH_2), 15.11 (CH_3). DEPT (90°) δ 131.55 (CH), 122.17 (CH), 119.07 (CH), 116.72 (CH), 116.59 (CH), 116.24 (CH), 113.69 (CH). HRMS (ESI+) *m/z*: 487.0953 (M + Na). HPLC purity = 97.334%, t_R = 5.508 min.

*4.3.15. 1-(4-(4-(Benzyloxy)phenoxy)phenyl)-2-((5-(3,4-dihydroxyphenyl)-1,3,4-oxadiazol-2-yl)thio)ethan-1-one (**16**)*

M.p. 226.6–228.3 °C. ^{1}H NMR (500 MHz, DMSO-d_6) δ 9.80 (s, 1H), 9.52 (s, 1H), 8.03 (d, *J* = 8.7 Hz, 2H), 7.45 (d, *J* = 7.4 Hz, 2H), 7.38 (t, *J* = 7.4 Hz, 2H), 7.32 (t, *J* = 7.2 Hz, 1H), 7.29 (s, 1H), 7.20 (d, *J* = 8.2, 1H), 7.08 (overlap, 4H), 6.99 (d, *J* = 8.7 Hz, 2H), 6.86 (d, *J* = 8.2 Hz, 1H), 5.09 (s, 2H), 5.03 (s, 2H). ^{13}C NMR (126 MHz, DMSO-d_6) δ 191.58 (s), 165.84 (s), 163.28 (s), 162.42 (s), 156.03 (s), 149.78 (s), 148.29 (s), 146.30 (s), 137.37 (s), 131.56 (s), 129.70 (s), 128.89 (s), 128.33 (s), 128.20 (s), 122.18 (s), 119.08 (s), 116.78 (s), 116.68 (s), 116.60 (s), 114.29 (s), 113.70 (s), 70.11 (s), 40.66 (s). DEPT (135°) δ 131.56 (CH), 128.89 (CH), 128.33 (CH), 128.20 (CH), 122.18 (CH), 119.08 (CH), 116.78 (CH), 116.68 (CH), 116.60 (CH), 113.70 (CH), 70.11 (negative peak, CH_2), 40.66 (negative peak, CH_2). DEPT (90°) δ 131.56 (CH), 128.89 (CH), 128.33 (CH), 128.20 (CH), 122.18 (CH), 119.08 (CH), 116.78 (CH), 116.68 (CH), 116.60 (CH), 113.70 (CH).

HRMS (ESI+) *m/z*: 549.1107 (M + Na). HPLC purity = 96.918%, t_R = 6.443 min.

4.3.16. 1-(4-(4-(Tert-butyl)phenoxy)phenyl)-2-((5-(3,4-dihydroxyphenyl)-1,3,4-oxadiazol-2-yl)thio)ethan-1-one (**17**)

M.p. 150.6–151.7 °C. ^{1}H NMR (500 MHz, DMSO-d_6) δ 9.79 (s, 1H), 9.51 (s, 1H), 8.05 (d, *J* = 8.6 Hz, 2H), 7.46 (d, *J* = 8.6 Hz, 2H), 7.29 (s, 1H), 7.20 (d, *J* = 8.2 Hz, 1H), 7.04 (overlap, 4H), 6.85 (d, *J* = 8.2 Hz, 1H), 5.04 (s, 2H), 1.28 (s, 9H). ^{13}C NMR (126 MHz, DMSO-d_6) δ 191.62 (s), 165.84 (s), 162.60 (s), 152.77 (s), 149.78 (s), 147.78 (s), 146.30 (s), 131.59 (s), 130.01 (s), 127.50 (s), 120.10 (s), 119.07 (s), 117.42 (s), 116.60 (s), 114.28 (s), 113.70 (s), 40.66 (s), 34.65 (s), 31.66 (s). DEPT (135°) δ 131.59 (CH), 127.50 (CH), 120.10 (CH), 119.07 (CH), 117.42 (CH), 116.60 (CH), 113.69 (CH), 40.66 (negative peak, CH_2), 31.66 (CH_3). DEPT (90°) δ 131.59 (CH), 127.50 (CH), 120.10 (CH), 119.08 (CH), 117.43 (CH), 113.70 (CH). HRMS (ESI+) *m/z*: 499.1312 (M + Na). HPLC purity = 95.853%, t_R = 3.592 min.

4.3.17. 2-((5-(3,4-Dihydroxyphenyl)-1,3,4-oxadiazol-2-yl)thio)-1-(4-(4-(2-methoxyethyl)phenoxy)phenyl)ethan-1-one (**18**)

M.p. 179.8–220.8 °C. ^{1}H NMR (500 MHz, DMSO-d_6) δ 9.79 (s, 1H), 9.51 (s, 1H), 8.05 (d, *J* = 8.7 Hz, 2H), 7.30 (overlap, 3H), 7.20 (d, *J* = 8.2 Hz, 1H), 7.04 (overlap, 4H), 6.85 (d, *J* = 8.2 Hz, 1H), 5.04 (s, 2H), 3.53 (t, *J* = 6.7 Hz, 2H), 3.23 (s, 3H), 2.81 (t, *J* = 6.7 Hz, 2H). ^{13}C NMR (126 MHz, DMSO-d_6) δ 191.61 (s), 165.84 (s), 162.61 (s), 162.42 (s), 153.34 (s), 149.78 (s), 146.30 (s), 136.37 (s), 131.58 (s), 131.08 (s), 130.01 (s), 120.44 (s), 119.08 (s), 117.40 (s), 116.60 (s), 114.28 (s), 113.70 (s), 73.06 (s), 58.27 (s), 40.66 (s), 35.04 (s). DEPT (135°) δ 131.58 (CH), 131.08 (CH), 120.44 (CH), 119.08 (CH), 117.40 (CH), 116.60 (CH), 113.70 (CH), 73.06 (negative peak, CH_2), 58.27 (CH_3), 40.67 (negative peak, CH_2), 35.04 (negative peak, CH_2). DEPT (90°) δ 131.58 (CH), 131.08 (CH), 120.44 (CH), 119.08 (CH), 117.40 (CH), 116.60 (CH), 113.69 (CH). HRMS (ESI+) *m/z*: 501.1113 (M + Na). HPLC purity = 95.371%, t_R = 4.973 min.

4.4. General procedure for the preparation of **19**–**27**

Copper(II) bromide (0.050 mol) and acetophenone (0.025 mol) to be brominated (0.03 mol) were placed in a flak fitted with a reflux condenser. Ethyl acetate (25 mL) and chloroform (25 mL) were added. The resulting reaction mixture was refluxed with vigorous stirring to ensure complete exposure of the copper(II) bromide to the reaction medium until the reaction was complete as judged by a color change of the solution from green to amber, disappearance of all black solid, and cessation of hydrogen bromide evolution. The copper(I) bromide was collected by filtration and washed well with ethyl acetate. The solvents were removed from the filtrate under reduced pressure. The resulting product, 2-bromoacetophenone, was purified by column chromatography on silica gel with petroleum ether and ethyl acetate (25:1) as the mobile phase.

A solution of 2-bromoacetophenone (0.0628 mol) and hexamethylenetetramine (9.67 g, 0.07 mmol) in $CHCl_3$ (50 mL) was stirred at room temperature for 2 h. The precipitated solid was filtered and washed with $CHCl_3$ to obtain quaternary ammonium compounds, which was used in the next step without further purification.

Concentrated HCl (30 mL) was dropped into the solution of quaternary ammonium in ethanol (100 mL). The reaction mixture was stirred at room temperature for 48 h. The white solid was removed by filtration and the filtrate was concentrated in vacuo. Recrystallization of the crude product yielded the desired product 2-aminoacetophenone as a white needle-like crystal.

To a DMF (10 mL) solution of aldehydes (2 mmol) were successively added 2-aminoacetophenone hydrochloride (4 mmol), iodine (0.6 mmol), TBHP (300 μL), $NaHCO_3$ (2 mmol). After the reaction mixture was stirred for 10 h at 70 °C, the reaction mixture was extracted with EtOAc, washed with diluted HCl followed by water, dried with Na_2SO_4. Then solvent was removed under reduced pressure and purified by silica gel column chromatography (CH_2Cl_2/MeOH = 40:1) to afford the desired product.

4.4.1. 4-(5-(4-Phenoxyphenyl)oxazol-2-yl)benzene-1,2-diol (**19**)

M.p. 209.1–210.6 °C. ^{1}H NMR (500 MHz, DMSO-d_6) δ 9.54 (s, 1H), 9.36 (s, 1H), 7.76 (d, *J* = 8.3 Hz, 2H), 7.62 (s, 1H), 7.48–7.37 (overlap, 3H), 7.36 (d, *J* = 8.2 Hz, 1H), 7.17 (t, *J* = 7.3 Hz, 1H), 7.09 (d, *J* = 8.3 Hz, 2H), 7.06 (d, *J* = 8.1 Hz, 2H), 6.85 (d, *J* = 8.2 Hz, 1H). ^{13}C NMR (126 MHz, DMSO-d_6) δ 161.04 (s), 157.13 (s), 156.63 (s), 149.85 (s), 148.59 (s), 146.09 (s), 130.61 (s), 126.11 (s), 124.31 (s), 123.64 (s), 123.47 (s), 119.42 (d), 118.57 (d), 116.46 (s), 113.58 (s). DEPT (135°) δ130.61 (CH), 126.11 (CH), 124.31 (CH), 123.64 (CH), 119.45 (CH), 119.38 (CH), 118.45 (CH), 116.46 (CH), 113.57 (CH). DEPT (90°) δ 130.61 (CH), 126.10 (CH), 124.31 (CH), 123.64 (CH), 119.45 (CH), 119.38 (CH), 118.45 (CH), 116.46 (CH), 113.57 (CH). HRMS (ESI+) *m/z*: 346.1073 (M + H). HPLC purity = 98.152%, t_R = 6.027 min.

4.4.2. 4-(5-(4-(p-tolyloxy)phenyl)oxazol-2-yl)benzene-1,2-diol (**20**)

M.p. 205.8–207.0 °C. ^{1}H NMR (600 MHz, DMSO-d_6) δ 9.58 (s, 1H), 9.40 (s, 1H), 7.79–7.73 (m, 2H), 7.62 (s, 1H), 7.44 (s, 1H), 7.38 (d, *J* = 8.2 Hz, 1H), 7.23 (d, *J* = 8.4 Hz, 2H), 7.08–7.05 (overlap, 2H), 6.98 (d, *J* = 8.4 Hz, 2H), 6.87 (d, *J* = 8.2 Hz, 1H), 2.30 (s, 3H). ^{13}C NMR (151 MHz, DMSO-d_6) δ 157.85 (s), 154.24 (s), 150.04 (s), 148.71 (s), 146.22 (s), 133.71 (s), 131.13 (s), 131.11 (s), 126.18 (s), 123.21 (s), 119.77 (s), 119.01 (s), 118.82 (s), 118.57 (s), 116.58 (s), 20.85 (s). DEPT (135°) δ 131.12 (CH), 126.18 (CH), 123.21 (CH), 119.77 (CH), 119.01 (CH), 118.82 (CH), 118.57 (CH), 116.58 (CH), 20.85 (CH_3). DEPT (90°) δ 131.11 (CH), 126.18 (CH), 123.21 (CH), 119.77 (CH), 119.01 (CH), 118.82 (CH), 118.57 (CH), 116.58 (CH). HRMS (ESI+) *m/z*: 360.1212 (M + H). HPLC purity = 99.000%, t_R = 4.994 min.

4.4.3. 4-(5-(4-(4-Methoxyphenoxy)phenyl)oxazol-2-yl)benzene-1,2-diol (**21**)

M.p. 236.9–238.1 °C. ^{1}H NMR (500 MHz, DMSO-d_6) δ 9.54 (s, 1H), 9.38 (s, 1H), 7.71 (d, *J* = 8.6 Hz, 2H), 7.58 (s, 1H), 7.43 (s, 1H), 7.36 (d, *J* = 8.2 Hz, 1H), 7.03 (d, *J* = 9.0 Hz, 2H), 7.00 (d, *J* = 8.6 Hz, 2H), 6.97 (d, *J* = 9.0 Hz, 2H), 6.85 (d, *J* = 8.2 Hz, 1H), 3.74 (s, 3H). ^{13}C NMR (126 MHz, DMSO-d_6) δ 160.93 (s), 158.48 (s), 156.32 (s), 149.95 (s), 149.33 (s), 148.55 (s), 146.08 (s), 126.01 (s), 123.34 (s), 122.70 (s), 121.40 (s), 118.72 (s), 118.43 (s), 118.13 (s), 116.46 (s), 115.61 (s), 113.56 (s), 55.86 (s). DEPT (135l) δ 126.01 (CH), 123.34 (CH), 121.40 (CH), 118.43 (CH), 118.13 (CH), 116.46 (CH), 115.61 (CH), 113.56 (CH), 55.86 (CH_3). DEPT (90°) δ 126.01 (CH), 123.34 (CH), 121.40 (CH), 118.43 (CH), 118.12 (CH), 116.46 (CH), 115.61 (CH), 113.55 (CH). HRMS (ESI+) *m/z*: 376.1164 (M + H). HPLC purity = 98.996%, t_R = 5.978 min.

4.4.4. 4-(5-(4-(4-(tert-butyl)phenoxy)phenyl)oxazol-2-yl)benzene-1,2-diol (**22**)

M.p. 202.4–204.5 °C. ^{1}H NMR (500 MHz, DMSO-d_6) δ 9.54 (s, 1H), 9.35 (s, 1H), 7.74 (d, *J* = 8.4 Hz, 2H), 7.60 (s, 1H), 7.45–7.37 (overlap, 3H), 7.35 (d, *J* = 8.1 Hz, 1H), 7.07 (d, *J* = 8.4 Hz, 2H), 6.97 (d, *J* = 8.4 Hz, 2H), 6.85 (d, *J* = 8.1 Hz, 1H), 1.27 (s, 9H). ^{13}C NMR (126 MHz, DMSO-d_6) δ 161.00 (s), 157.41 (s), 154.18 (s), 149.89 (s), 148.57 (s), 146.65 (s), 146.08 (s), 127.24 (s), 126.06 (s), 123.54 (s), 123.24 (s), 119.20 (s), 118.95 (s), 118.69 (s), 118.43 (s), 116.45 (s), 113.56 (s), 34.54 (s), 31.69 (s). DEPT (135°) δ 127.24 (CH), 126.07 (CH), 123.54 (CH), 119.20 (CH), 118.95 (CH), 118.43 (CH), 116.45 (CH), 113.56 (CH), 31.69 (CH_3). DEPT (90°) δ 127.24 (CH), 126.06 (CH), 123.54 (CH), 119.19 (CH), 118.95 (CH), 118.43 (CH), 116.45 (CH),

113.56 (CH). HRMS (ESI+) *m/z*: 402.1687 (M + H). HPLC purity = 96.681%, t_R = 7.809 min.

4.4.5. 4-(5-(4-([1,1′-Biphenyl]-4-yloxy)phenyl)oxazol-2-yl) benzene-1,2-diol (**23**)

M.p. 263.2–234.2 °C. ^{1}H NMR (500 MHz, DMSO-d_6) δ 9.56 (s, 1H), 9.37 (s, 1H), 7.78 (d, *J* = 8.6 Hz, 2H), 7.68 (d, *J* = 8.6 Hz, 2H), 7.63 (overlap, 3H), 7.45 (s, 1H), 7.43 (t, *J* = 8.3 Hz, 2H), 7.38 (d, *J* = 8.2 Hz, 1H), 7.32 (t, *J* = 8.3 Hz, 1H), 7.15 (d, *J* = 8.7 Hz, 2H), 7.12 (d, *J* = 8.7 Hz, 2H), 6.86 (d, *J* = 8.2 Hz, 1H). ^{13}C NMR (126 MHz, DMSO-d_6) δ 161.09 (s), 156.93 (s), 156.36 (s), 149.84 (s), 148.61 (s), 146.11 (s), 139.83 (s), 136.16 (s), 129.37 (s), 128.81 (s), 127.67 (s), 126.91 (s), 126.14 (s), 123.72 (s), 123.68 (s), 119.71 (s), 119.63 (s), 118.70 (s), 118.48 (s), 116.48 (s), 113.60 (s). DEPT (135°) δ 129.37 (CH), 128.81 (CH), 127.66 (CH), 126.91 (CH), 126.14 (CH), 123.71 (CH), 119.71 (CH), 119.63 (CH), 118.48 (CH), 116.47 (CH), 113.60 (CH). DEPT (90°) δ 129.37 (CH), 128.81 (CH), 127.67 (CH), 126.91 (CH), 126.14 (CH), 123.72 (CH), 119.71 (CH), 119.63 (CH), 118.48 (CH), 116.47 (CH), 113.60 (CH). HRMS (ESI+) *m/z*: 444.1187 (M + Na). HPLC purity = 98.458%, t_R = 5.957 min.

4.4.6. 4-(5-(4-(4-Isopropylphenoxy)phenyl)oxazol-2-yl)benzene-1,2-diol (**24**)

M.p. 196.1–196.8 °C. ^{1}H NMR (500 MHz, DMSO-d_6) δ 9.53 (s, 1H), 9.35 (s, 1H), 7.74 (d, *J* = 8.7 Hz, 2H), 7.60 (s, 1H), 7.42 (s, 1H), 7.35 (d, *J* = 8.2 Hz, 1H), 7.26 (d, *J* = 8.5 Hz, 2H), 7.06 (d, *J* = 8.7 Hz, 2H), 6.98 (d, *J* = 8.5 Hz, 2H), 6.84 (d, *J* = 8.2 Hz, 1H), 2.87 (m, 1H), 1.19 (d, *J* = 6.9 Hz, 6H). ^{13}C NMR (126 MHz, DMSO-d_6) δ 160.99 (s), 157.50 (s), 154.43 (s), 149.89 (s), 148.57 (s), 146.08 (s), 144.42 (s), 128.29 (s), 126.07 (s), 123.53 (s), 123.20 (s), 119.38 (s), 119.13 (s), 118.69 (s), 118.43 (s), 116.45 (s), 113.56 (s), 33.22 (s), 24.43 (s). DEPT (135°) δ 128.29 (CH), 126.06 (CH), 123.53 (CH), 119.38 (CH), 119.12 (CH), 118.43 (CH), 116.45 (CH), 113.56 (CH), 33.21 (CH), 24.42 (CH_3). DEPT (90°) δ 128.29 (CH), 126.07 (CH), 123.53 (CH), 119.38 (CH), 119.13 (CH), 118.43 (CH), 116.45 (CH), 113.56 (CH), 33.22 (CH). HRMS (ESI+) *m/z*: 410.1349 (M + Na). HPLC purity = 97.981%, t_R = 7.449 min.

4.4.7. 4-(5-(4-(4-(tert-pentyl)phenoxy)phenyl)oxazol-2-yl) benzene-1,2-diol (**25**)

M.p. 218.4–219.6 °C. ^{1}H NMR (500 MHz, DMSO-d_6) δ 9.45 (overlap, 2H), 7.74 (d, *J* = 8.7 Hz, 2H), 7.60 (s, 1H), 7.42 (s, 1H), 7.35 (overlap, 3H), 7.06 (d, *J* = 8.6 Hz, 2H), 6.98 (d, *J* = 8.6 Hz, 2H), 6.84 (d, *J* = 8.2 Hz, 1H), 1.58 (t, *J* = 7.4 Hz, 2H), 1.23 (s, 6H), 0.62 (t, *J* = 7.4 Hz, 3H). ^{13}C NMR (126 MHz, DMSO-d_6) δ 161.00 (s), 157.42 (s), 154.11 (s), 149.89 (s), 148.58 (s), 146.09 (s), 144.91 (s), 127.87 (s), 126.07 (s), 123.54 (s), 123.24 (s), 119.20 (s), 118.91 (s), 118.68 (s), 118.43 (s), 116.45 (s), 113.57 (s), 37.70 (s), 36.69 (s), 28.77 (s), 9.51 (s). DEPT (135°) δ 127.87 (CH), 126.07 (CH), 123.54 (CH), 119.20 (CH), 118.90 (CH), 118.43 (CH), 116.45 (CH), 113.56 (CH), 36.68 (CH), 28.76 (negative peak, CH_2), 9.51 (CH_3). DEPT (90°) δ 127.87 (CH), 126.07 (CH), 123.54 (CH), 119.20 (CH), 118.90 (CH), 118.43 (CH), 116.45 (CH), 113.56 (CH), 40.23 (CH), 36.69 (CH). HRMS (ESI+) *m/z*: 416.1850 (M + H). HPLC purity = 99.160%, t_R = 9.472 min.

4.4.8. 4-(5-(4-(4-Ethoxyphenoxy)phenyl)oxazol-2-yl)benzene-1,2-diol (**26**)

M.p. 225.9–227.1 °C. ^{1}H NMR (500 MHz, DMSO-d_6) δ 9.53 (s, 1H), 9.35 (s, 1H), 7.71 (d, *J* = 8.8 Hz, 2H), 7.58 (s, 1H), 7.41 (s, 1H), 7.35 (d, *J* = 8.2 Hz, 1H), 7.06–6.97 (overlap, 4H), 6.95 (d, *J* = 8.2 Hz, 2H), 6.84 (d, *J* = 8.2 Hz, 1H), 4.00 (q, *J* = 7.0 Hz, 2H), 1.31 (t, *J* = 7.0 Hz, 3H). ^{13}C NMR (126 MHz, DMSO-d_6) δ 160.92 (s), 158.48 (s), 155.61 (s), 149.94 (s), 149.22 (s), 148.54 (s), 146.07 (s), 126.01 (s), 123.35 (s), 122.69 (s), 121.38 (s), 118.70 (s), 118.41 (s), 118.14 (s), 116.45 (s), 116.10 (s), 113.54 (s), 63.83 (s), 15.14 (s). DEPT (135°) δ 126.01 (CH), 123.35 (CH), 121.38 (CH), 118.41 (CH), 118.13 (CH), 116.45 (CH), 116.10 (CH), 113.54 (CH), 63.83 (negative peak, CH_2), 15.14 (CH_3). DEPT (90°) δ 126.01 (CH), 123.35 (CH), 121.38 (CH), 118.41 (CH), 118.13 (CH), 116.44 (CH), 116.10 (CH), 113.54 (CH). HRMS (ESI+) *m/z*: 390.1329 (M + H). HPLC purity = 99.181%, t_R = 6.547 min.

4.4.9. 4-(5-(4-(4-(2-Methoxyethyl)phenoxy)phenyl)oxazol-2-yl) benzene-1,2-diol (**27**)

M.p. 142.7–144.0 °C. ^{1}H NMR (500 MHz, DMSO-d_6) δ 9.53 (s, 1H), 9.35 (s, 1H), 7.74 (d, *J* = 8.7 Hz, 2H), 7.60 (s, 1H), 7.42 (s, 1H), 7.35 (d, *J* = 8.2 Hz, 1H), 7.25 (d, *J* = 8.5 Hz, 2H), 7.06 (d, *J* = 8.7 Hz, 2H), 6.97 (d, *J* = 8.5 Hz, 2H), 6.84 (d, *J* = 8.2 Hz, 1H), 3.52 (d, *J* = 6.8 Hz, 2H), 3.23 (s, 3H), 2.78 (t, *J* = 6.8 Hz, 2H). ^{13}C NMR (126 MHz, DMSO-d_6) δ 161.00 (s), 157.45 (s), 154.75 (s), 149.88 (s), 148.57 (s), 146.08 (s), 135.20 (s), 130.86 (s), 126.07 (s), 123.55 (s), 123.24 (s), 119.34 (s), 119.15 (s), 118.68 (s), 118.43 (s), 116.45 (s), 113.56 (s), 73.16 (s), 58.26 (s), 35.01 (s). DEPT (135°) δ 130.86 (CH), 126.06 (CH), 123.55 (CH), 119.34 (CH), 119.15 (CH), 118.43 (CH), 116.45 (CH), 113.55 (CH), 73.16 (negative peak, CH_2), 58.26 (CH_3), 35.00 (negative peak, CH_2). DEPT (90°) δ 130.86 (CH), 126.07 (CH), 123.55 (CH), 119.34 (CH), 119.15 (CH), 118.43 (CH), 116.45 (CH), 113.56 (CH). HRMS (ESI+) *m/z*: 426.1305 (M + Na). HPLC purity = 99.033%, t_R = 3.197 min.

4.5. Enzyme inhibition assays

The PTP1B enzyme reaction was carried out under the conditions described previously [44]. The effect of each compound on the PTP1B-catalyzed pNPP hydrolysis was determined at 37 °C and pH 7.5 in a 100 μL reaction system in a 96-well plate. Each reaction contained 1 μL compound in DMSO (final concentration from 100 to 0.01 μM) and 99 μL assay buffer (10 mM Tris-HCl, 25 mM NaCl, 1 mM EDTA and 2 mM DTT) containing 4 mM pNPP and 60 nM PTP1B. The PTP1B-catalyzed reaction was started by addition of the PTP1B and terminated by the addition of 1 N NaOH after 30 min. The amount of product *p*-nitrophenol was determined from the absorbance at 405 nm detected by a SpectraMAX Plus 384 microplate pectrophotometer. The IC_{50} value was obtained by plotting relative PTP1B activity versus inhibitor concentration and fitting to equation %Inhibition = Bottom + (Top-Bottom)/(1 + $10^{(lgIC50-X)*h}$).

4.6. Docking studies

The crystal structure of the PTP1B (PDB ID: 1G1H) was obtained from the protein bank in the RCSB. The 3D structures of the inhibitors were generated using Chembio3D Ultra 11.0 followed by energy minimization. AutoDock 4.0 program equipped with ADT was used to perform the automated molecular docking. Grid maps covering residues in the catalytic site were defined for all inhibitors in the AutoDock calculations using a grid spacing of 60 Å. The GA-LS algorithm was adopted using default settings. For each docking job, 200 hybrid GA-LS runs were carried-out. A total of 200 possible binding conformations were generated and grouped into clusters based on a 1.0 Å cluster tolerance. The docking models were analyzed and represented using ADT.

4.7. Cell culture and differentiation

A mouse muscle myoblasts cell line (C2C12) was obtained from American Type Culture Collection (Rockville, MD) and was cultured in DMEM supplemented with 10% fetal calf serum and 1% penicillin-streptomycin and incubated in an atmosphere of 95% O_2 and 5% CO_2 in air. After confluence, the culture medium was replaced with DMEM containing 10% horse serum to initiate myogenic differentiation [45]. After differentiation, myotubes were subjected to various treatment described below.

C2C12 myotubes were starved in serum-free DMEM for 24 h,

after exchanged with fresh serum-freemedium, then they were exposed to each concentration of compound **22**. Insulin resistance was induced in C2C12 myotubes by treating them with palmitic acid (PA) (0.75 mM) for 16 h. PA was prepared by conjugating it with bovine serum albumin as previously reported and bovine serum albumin was included in the cell culture medium for every condition tested as a control. PA were added when C2C12 myotubes had been pre-incubated with compound **22** for 1 h.

Normal C2C12 myotubes and insulin-resistant C2C12 in 6-well plates were treated with different concentration. After stimulating with 10 nM or 100 nM insulin for 30 min at 37 °C, the cells were washed with ice-cold PBS and then lysed with RIPA lysis buffer (strong) on ice for 5 min. Insoluble material was removed by centrifugation at 12000 rpm for 10 min. The protein concentrations were determined by Beyotime protein assay kit and stored at −80 °C until the Western blotting analyses.

Total proteins (10 μg) were electrophoresed on SDS polyacrylamide gels, and then transferred to PVDF membranes. Membranes were blocked in blocking buffer and then incubated with primary antibodies overnight at 4 °C, followed by incubation with appropriate secondary antibodies for 1 h at room temperature. Membranes were washed three times with TBST for 5 min each time. Finally, the chemiluminescence method was employed to detect the signals using Pierce™ ECL Western Blotting Substrate (Thermo Scientific, Waltham, MA, USA) and protein bands were visualized by autoradiography and the intensities were analyzed by Image J public domain software from the National Institutes of Health(Bethesda, MD, USA). Comparisons were made between average values only of bands within the same gel.

Acknowledgment

This work was supported by the National Natural Science Foundation of China (No. 41506169), and Key research and development project of Shandong province (2015GSF115029, 2016ZDJS07A13, 2016GSF115002, 2016ZDJS07A13, 2016GSF201193), and Key Research Program of Frontier Sciences, CAS (QYZDB-SSW-DQC014), and China Postdoctoral Science Foundation (2015KY11-4), and the Project of Discovery, Evaluation and Transformation of Active Natural Compounds, Strategic Biological Resources Service Network Programme of Chinese Academy of Sciences (ZSTH-026), and NSFC-Shandong Joint Fund for Marine Science Rearch Centers (U1606403), and the Scientific and Technological Innovation Project Financially Supported by Qingdao National Laboratory for Marine Science and Technology (No. 2015ASKJ02), and Aoshan Talents Program Supported by Qingdao National Laboratory for Marine Science and Technology (NO. 2015ASTP), and National Program for Support of Top-notch Young Professionals, and Taishan scholar Youth Project of Shandong province.

Appendix A. Supplementary data

Supplementary data related to this article can be found at http://dx.doi.org/10.1016/j.ejmech.2017.05.007.

ABBREVIATIONS

PTP1B	Protein tyrosine phosphatase 1B
TCPTP	T-cell protein tyrosine phosphatase
TBHP	*tert*-Butyl hydroperoxide
pNPP	disodium 4-nitrophenyl phosphate

References

[1] L. Zhang, C.S. Jiang, L.X. Gao, J.X. Gong, Z.H. Wang, J.Y. Li, J. Li, X.W. Li, Y.W. Guo, Design, synthesis and in vitro activity of phidianidine B derivatives as novel PTP1B inhibitors with specific selectivity, Bioorg. Med. Chem. Lett. 26 (2016) 778–781.
[2] B.J. Goldstein, Protein-tyrosine phosphatase 1B (PTP1B): a novel therapeutic target for type 2 diabetes mellitus, obesity and related states of insulin resistance, Curr. Drug. Targets 1 (2001) 265–275.
[3] A.B. Comeau, D.A. Critton, R. Page, C.T. Seto, A focused library of protein tyrosine phosphatase inhibitors, J. Med. Chem. 53 (2010) 6768–6772.
[4] K.A. Kenner, E. Anyanwu, J.M. Olefsky, J. Kusari, Protein-tyrosine phosphatase 1B is a negative regulator of insulin-and insulin-like growth factor-I-stimulated signaling, J. Biol. Chem. 271 (1996) 19810–19816.
[5] M. Elchebly, P. Payette, E. Michaliszyn, W. Cromlish, S. Collins, A.L. Loy, D. Normandin, A. Cheng, J. Himms-Hagen, C.C. Chan, C. Ramachandran, M.J. Gresser, M.L. Tremblay, B.P. Kennedy, Increased insulin sensitivity and obesity resistance in mice lacking the protein tyrosine phosphatase-1B gene, Science 283 (1999) 1544–1548.
[6] L.D. Klaman, O. Boss, O.D. Peroni, J.K. Kim, J.L. Martino, J.M. Zabolotny, N. Moghal, M. Lubkin, Y.B. Kim, A.H. Sharpe, A. Stricker-Krongrad, G.I. Shulman, B.G. Neel, B.B. Kahn, Increased energy expenditure, decreased adiposity, and tissue-specific insulin sensitivity in protein-tyrosine phosphatase 1B-deficient mice, Mol. Cell Biol. 20 (2000) 5479–5489.
[7] I.G. Boutselis, X. Yu, Z.-Y. Zhang, R.F. Borch, Synthesis and cell-based activity of a potent and selective protein tyrosine phosphatase 1B inhibitor prodrug, J. Med. Chem. 50 (2007) 856–864.
[8] Y.A. Puius, Y. Zhao, M. Sullivan, D.S. Lawrence, S.C. Almo, Z.-Y. Zhang, Identification of a second aryl phosphate-binding site in protein-tyrosine phosphatase 1B: a paradigm for inhibitor design, Proc. Natl. Acad. Sci. 94 (1997) 13420–13425.
[9] D.P. Wilson, Z.-K. Wan, W.-X. Xu, S.J. Kirincich, B.C. Follows, D. Joseph-McCarthy, K. Foreman, A. Moretto, J. Wu, M. Zhu, Structure-based optimization of protein tyrosine phosphatase 1B inhibitors: from the active site to the second phosphotyrosine binding site, J. Med. Chem. 50 (2007) 4681–4698.
[10] G. Liu, Z. Xin, Z. Pei, P.J. Hajduk, C. Abad-Zapatero, C.W. Hutchins, H. Zhao, T.H. Lubben, S.J. Ballaron, D.L. Haasch, Fragment screening and assembly: a highly efficient approach to a selective and cell active protein tyrosine phosphatase 1B inhibitor, J. Med. Chem. 46 (2003) 4232–4235.
[11] M.A.T. Blaskovich, Drug discovery and protein tyrosine phosphatases, Curr. Med. Chem. 16 (2009) 2095–2176.
[12] A.P. Combs, Recent advances in the discovery of competitive protein tyrosine phosphatase 1B inhibitors for the treatment of diabetes, obesity, and cancer, J. Med. Chem. 53 (2010) 2333–2344.
[13] K.A. Lantz, S.G.E. Hart, S.L. Planey, M.F. Roitman, I.A. Ruiz-White, H.R. Wolfe, M.P. McLane, Inhibition of PTP1B by trodusquemine (MSI-1436) causes fat-specific weight loss in diet-induced obese mice, Obesity 18 (2010) 1516–1523.
[14] G. Liu, Z. Xin, H. Liang, C. Abad-Zapatero, P.J. Hajduk, D.A. Janowick, B.G. Szczepankiewicz, Z. Pei, C.W. Hutchins, S.J. Ballaron, Selective protein tyrosine phosphatase 1B inhibitors: targeting the second phosphotyrosine binding site with non-carboxylic acid-containing ligands, J. Med. Chem. 46 (2003) 3437–3440.
[15] K.E. You-Ten, E.S. Muise, A. Itié, E. Michaliszyn, J. Wagner, S. Jothy, W.S. Lapp, M.L. Tremblay, Impaired bone marrow microenvironment and immune function in T cell protein tyrosine phosphatase–deficient mice, J. Exp. Med. 186 (1997) 683–693.
[16] X. Li, L. Wang, D. Shi, The design strategy of selective PTP1B inhibitors over TCPTP, Bioorgan. Med. Chem. 24 (2016) 3343–3352.
[17] Y.T. Chen, C.T. Seto, Parallel synthesis of a library of bidentate protein tyrosine phosphatase inhibitors based on the alpha-ketoacid motif, Bioorg. Med. Chem. 12 (2004) 3289–3298.
[18] H.S. Andersen, O.H. Olsen, L.F. Iversen, A.L. Sørensen, S.B. Mortensen, M.S. Christensen, S. Branner, T.K. Hansen, J.F. Lau, L. Jeppesen, Discovery and SAR of a novel selective and orally bioavailable nonpeptide classical competitive inhibitor class of protein-tyrosine phosphatase 1B, J. Med. Chem. 45 (2002) 4443–4459.
[19] A.P. Combs, E.W. Yue, M. Bower, P.J. Ala, B. Wayland, B. Douty, A. Takvorian, P. Polam, Z. Wasserman, W. Zhu, Structure-based design and discovery of protein tyrosine phosphatase inhibitors incorporating novel isothiazolidinone heterocyclic phosphotyrosine mimetics, J. Med. Chem. 48 (2005) 6544–6548.
[20] A.P. Combs, W. Zhu, M.L. Crawley, B. Glass, P. Polam, R.B. Sparks, D. Modi, A. Takvorian, E. McLaughlin, E.W. Yue, Z. Wasserman, M. Bower, M. Wei, M. Rupar, P.J. Ala, B.M. Reid, D. Ellis, L. Gonneville, T. Emm, N. Taylor, S. Yeleswaram, Y. Li, R. Wynn, T.C. Burn, G. Hollis, P.C.C. Liu, B. Metcalf, Potent benzimidazole sulfonamide protein tyrosine phosphatase 1B inhibitors containing the heterocyclic (S)-Isothiazolidinone phosphotyrosine mimetic, J. Med. Chem. 49 (2006) 3774–3789.
[21] X. Fan, N.J. Xu, J.G. Shi, Bromophenols from the red alga rhodomela confervoides, J. Nat. Prod. 66 (2003) 455–458.
[22] D. Shi, F. Xu, J. He, J. Li, X. Fan, L. Han, Inhibition of bromophenols against PTP1B and anti-hyperglycemic effect of Rhodomela confervoides extract in diabetic rats, Chin. Sci. Bull. 53 (2008) 2476–2479.
[23] R.M. Chen, L.H. Hu, T.Y. An, J. Li, Q. Shen, Natural PTP1B Inhibitors from

broussonetia papyrifera, Bioorg. Med. Chem. Lett. 12 (2002) 3387–3390.
[24] W. Li, S. Li, K. Higai, T. Sasaki, Y. Asada, S. Ohshima, K. Koike, Evaluation of licorice flavonoids as protein tyrosine phosphatase 1B inhibitors, Bioorg. Med. Chem. Lett. 23 (2013) 5836–5839.
[25] Q.H. Vo, P.H. Nguyen, B.T. Zhao, M.Y. Ali, J.S. Choi, B.S. Min, T.H. Nguyen, M.H. Woo, Protein tyrosine phosphatase 1B (PTP1B) inhibitory constituents from the aerial parts of Tradescantia spathacea Sw, Fitoterapia 103 (2015) 113–121.
[26] Y. Wang, X.-Y. Shang, S.-J. Wang, S.-Y. Mo, S. Li, Y.-C. Yang, F. Ye, J.-G. Shi, L. He, Structures, biogenesis, and biological activities of pyrano[4,3-c]isochromen-4-one derivatives from the fungus Phellinus igniarius, J. Nat. Prod. 70 (2007) 296–299.
[27] J.R. Reid, N.D. Heindel, Improved syntheses of 5-substituted-4-amino-3-mercapto-(4 H)-1,2,4-triazoles, J. Heterocycl. Chem. 13 (1976) 925–926.
[28] T. Miao, L. Wang, Immobilization of copper in organic-inorganic hybrid materials: a highly efficient and reusable catalyst for the Ullmann diaryl etherification, Tetrahedron Lett. 48 (2007) 95–99.
[29] L.C. King, G.K. Ostrum, Selective bromination with copper(II) bromide, J. Org. Chem. 29 (1964) 3459–3461.
[30] P. Yu, Synthesis of α-aminoacetophenone hydrochloride and its p-substituted derivatives, Chem. Reag. 8 (1986) 302–305.
[31] C. Wan, L. Gao, Q. Wang, J. Zhang, Z. Wang, Simple and efficient preparation of 2, 5-disubstituted oxazoles via a metal-free-catalyzed cascade cyclization, Org. Lett. 12 (2010) 3902–3905.
[32] J. Liu, F. Jiang, Y. Jin, Y. Zhang, J. Liu, W. Liu, L. Fu, Design, synthesis, and evaluation of 2-substituted ethenesulfonic acid ester derivatives as protein tyrosine phosphatase 1B inhibitors, Eur. J. Med. Chem. 57 (2012) 10–20.
[33] R. Ottana, R. Maccari, S. Amuso, G. Wolber, D. Schuster, S. Herdlinger, G. Manao, G. Camici, P. Paoli, New 4-[(5-arylidene-2-arylimino-4-oxo-3-thiazolidinyl)methyl]benzoic acids active as protein tyrosine phosphatase inhibitors endowed with insulinomimetic effect on mouse C2C12 skeletal muscle cells, Eur. J. Med. Chem. 50 (2012) 332–343.
[34] A.P. Chandrasekharappa, S.E. Badiger, P.K. Dubey, S.K. Panigrahi, S.R.V. Manukonda, Design and synthesis of 2-substituted benzoxazoles as novel PTP1B inhibitors, Bioorg. Med. Chem. Lett. 23 (2013) 2579–2584.
[35] Y. Zhi, L.-X. Gao, Y. Jin, C.-L. Tang, J.-Y. Li, J. Li, Y.-Q. Long, 4-Quinolone-3-carboxylic acids as cell-permeable inhibitors of protein tyrosine phosphatase 1B, Bioorgan. Med. Chem. 22 (2014) 3670–3683.
[36] D. Ye, Y. Zhang, F. Wang, M. Zheng, X. Zhang, X. Luo, X. Shen, H. Jiang, H. Liu, Novel thiophene derivatives as PTP1B inhibitors with selectivity and cellular activity, Bioorgan. Med. Chem. 18 (2010) 1773–1782.
[37] G.G. Ferenczy, G.M. Keseru, Thermodynamics guided lead discovery and optimization, Drug Discov. Today 15 (2010) 919–932.
[38] P.R. Andrews, D.J. Craik, J.L. Martin, Functional group contributions to drug-receptor interactions, J. Med. Chem. 27 (1984) 1648–1657.
[39] E. Freire, Do enthalpy and entropy distinguish first in class from best in class? Drug Discov. Today 13 (2008) 869–874.
[40] T.S.G. Olsson, M.A. Williams, W.R. Pitt, J.E. Ladbury, The thermodynamics of protein–ligand interaction and solvation: insights for ligand design, J. Mol. Biol. 384 (2008) 1002–1017.
[41] A. Maeda, K. Kai, M. Ishii, T. Ishii, M. Akagawa, Safranal, a novel protein tyrosine phosphatase 1B inhibitor, activates insulin signaling in C2C12 myotubes and improves glucose tolerance in diabetic KK-Ay mice, Mol. Nutr. food Res. 58 (2014) 1177–1189.
[42] Z.-Q. Liu, T. Liu, C. Chen, M.-Y. Li, Z.-Y. Wang, R.-s. Chen, G.-x. Wei, X.-y. Wang, D.-Q. Luo, Fumosorinone, a novel PTP1B inhibitor, activates insulin signaling in insulin-resistance HepG2 cells and shows anti-diabetic effect in diabetic KKAy mice, Toxicol. Appl. Pharm. 285 (2015) 61–70.
[43] X. Zhang, J. Tian, J. Li, L. Huang, S. Wu, W. Liang, L. Zhong, J. Ye, F. Ye, A novel protein tyrosine phosphatase 1B inhibitor with therapeutic potential for insulin resistance, Brit. J. Pharmacol. 173 (2016) 1939–1949.
[44] T. Sun, Q. Wang, Z. Yu, Y. Zhang, Y. Guo, K. Chen, X. Shen, H. Jiang, Hyrtiosal, a PTP1B inhibitor from the marine sponge hyrtios erectus, shows extensive cellular effects on PI3K/AKT activation, glucose transport, and TGFβ/smad2 signaling, Chembiochem 8 (2007) 187–193.
[45] T. Nedachi, M. Kanzaki, Regulation of glucose transporters by insulin and extracellular glucose in C2C12 myotubes, Am. J. Physiol-endoc. M. 291 (2006) 817–828.